Spectra of one-dimensional excitons in polysilanes with various backbone conformations

H. Tachibana and M. Matsumoto
National Institute of Materials and Chemical Research, Tsukuba, Ibaraki 305, Japan

Y. Tokura, Y. Moritomo, A. Yamaguchi,* and S. Koshihara†
Department of Physics, University of Tokyo, Tokyo 113, Japan

R. D. Miller
IBM Research Division, Almaden Research Center, San Jose, California 95120-6099

S. Abe
Electrotechnical Laboratory, Tsukuba, Ibaraki 305, Japan
(Received 3 September 1992)

Linear and nonlinear optical spectra (one-photon and two-photon absorption, photoluminescence, and electroabsorption spectra) have been investigated for solid thin films of polysilanes with a variety of conformations, such as *trans*-planar, alternating *trans-gauche* (TGTG′ type), $\frac{7}{3}$ helical, and disordered backbone structures. Optical spectra have revealed features of one-dimensional exciton states characteristic of the respective conformations. In particular, the lowest allowed and second parity-forbidden (or two-photon allowed) transitions can be assigned to the ground ($^1B_{1u}$) and first excited (^1A_g) states of one-dimensional Wannier-type exciton, respectively. Furthermore, the higher excited exciton states and subsequent band-to-band transitions show up in the electroabsorption spectra for polysilanes with various conformations of the Si backbones. Quantitative analysis based on a microscopic theory for the one-dimensional excitons is also presented.

I. INTRODUCTION

Polysilanes are σ-electron-conjugated Si polymers that have a fairly wide electronic gap (3–4 eV).[1–3] A number of interesting photoelectronic properties have been found in polysilanes, e.g., fairly large third-order nonlinear optical susceptibility,[4] photoluminescence with high quantum efficiency (>0.1),[5] hole transport with high mobility,[6] and photosensitive functionality as self-developing photoresists.[7] The backbones of polysilanes take a variety of conformations such as *trans*-planar, alternating *trans-gauche* (TGTG′-type), $\frac{7}{3}$ helical, and disordered forms, depending on alkyl substituents attached to the polymer backbones. Furthermore, most of regular Si-backbone conformations undergo an order-disorder-type phase transition at elevated temperatures. The electronic structures (and hence optical properties) or polysilanes should depend significantly on the conformation structures of the backbone.

As far as the electronic structure of the Si backbones is concerned, an ideally ordered polysilane backbone may be viewed as an ultimate quantum wire made of Si. Identification of excitons and band-to-band transitions on such a Si wire is of current interest from the viewpoint of a one-dimensional semiconductor. Recently, distinct two-photon transitions on the higher-energy side of the intense one-photon absorption bands in various polysilanes have been detected by two-photon absorption[8–11] and electroabsorption[12,13] spectroscopy. Fairly sharp one-photon and two-photon absorption bands have been interpreted in terms of exciton transitions and not band-to-band transitions. The exciton states and electron-hole continuum in one-dimensional electronic systems such as polysilanes are considered to differ significantly from those in the conventional three-dimensional semiconductors.

In this paper, we have spectroscopically investigated the conformation dependence of electronic states in solid films of poly(di-*n*-hexylsilane) (PDHS), poly(di-*n*-tetradecylsilane) (PDTDS), poly(di-*n*-butylsilane) (PDBS), and poly(methyl-4-methylpentylsilane) (PMMPS), which show the prototypical conformations of polymer backbones (see Fig. 1 and Table I); *trans*-planar, alternating *trans-gauche* (TGTG′ type), $\frac{7}{3}$ helical, and disordered conformations, respectively.[3] The first three polysilanes undergo the above-mentioned order-disorder phase transitions at elevated temperatures, while polysilane chains

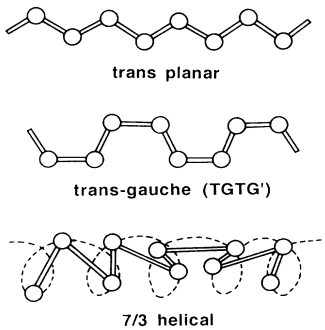

FIG. 1. Various backbone conformations in polysilanes.

TABLE I. Sidechains, conformations, and molecular weights of various polysilanes investigated in the present work.

	$-(R_1R_2Si)_n-$	Backbone conformation	Transition temperature (K)	Molecular weight (M_w)
PDHS	$R_1=R_2=n$-hexyl	*trans*-planar–disordered	315	2.44×10^5
PDTDS	$R_1=R_2=n$-tetradecyl	*trans*-gauche–disordered	328	4.66×10^5
PDBS	$R_1=R_2=n$-butyl	$\frac{7}{3}$ helical–disordered	356	1.92×10^5
PMMPS	R_1=methyl R_2=4-methylpentyl	disordered		1.18×10^5

with branched alkyl substituents, e.g., PMMPS, remain disordered even at low temperatures. Electronic structures of these polysilanes have been investigated by measurements of one-photon and two-photon absorption, photoluminescence, and electroabsorption spectra. The two-photon absorption spectroscopy can probe parity-forbidden states that cannot be detected by the ordinary (one-photon) absorption. In addition, the electroabsorption spectra can also pick up very weak (or blurred) transitions (of both parity-allowed and -forbidden states) buried in the absorption continuum that are hard to detect by ordinary absorption spectroscopy. We have revealed quantitative features in one-dimensional exciton states associated with the interband transitions between the σ-electron bands and their dependence on the conformation of the backbones. Preliminary results (mainly two-photon absorption spectra and a part of the electroabsorption spectra) have been published previously in short papers.[11,12,14] In the present paper, we comprehensively investigate various linear and nonlinear optical spectra and analyze them in terms of the unified picture of one-dimensional Wannier exciton states.

II. EXPERIMENT

A. Sample preparation

The respective polysilanes were synthesized by Wurtz coupling reaction of the corresponding dichloroalkylsilanes with sodium as described in the literature.[15,16] The molecular weights of the polymers relative to polystyrene standards were determined by gel permeation chromatography. Weight-average molecular weights (M_W) of the respective polysilanes are also listed in Table I. Thin solid films were prepared by coating from heptane solutions on fused quartz plates. The film thicknesses (ca. 110 nm) were determined by the tallystep method. The cast films were heated at 380 K for 15 min and were allowed to stand overnight at room temperature. For the purpose of the electroabsorption measurements, polysilanes were cast on the (indium-tinoxide)-coated quartz plates and a semitransparent aluminum electrode was vacuum deposited as a counter electrode on top of the thin film.

B. Optical measurements

Photoluminescence spectra were measured using 308-nm (4.0-eV) light from a XeCl excimer laser as an excitation source. Two-photon absorption spectra were recorded by monitoring the intensity of two-photon induced photoluminescence as a function of twice the photon energy of the exciting laser pulse. A pulse dye laser driven by a XeCl excimer laser was utilized as an excitation source. The intensity of the two-photon induced photoluminescence was confirmed to be precisely proportional to the square of the exciting laser intensity at several photon energies.

For measurements of electroabsorption spectra, sinusoidal electric field ($f=1$ KHz) was applied normal to the films and the modulated signals were detected at a frequency of $2f$ with a lock-in amplifier. Intensities of the electroabsorption signals varied quadratically with the applied field strength.

III. CONFORMATION DEPENDENCE OF ABSORPTION AND PHOTOLUMINESCENCE SPECTRA

Figure 2 shows ordinary (one-photon) absorption (OA) and photoluminescence (PL) spectra at 77 K for thin films of PDHS, PDTDS, and PDBS. For comparison, the OA spectra for the disordered conformation at higher temperatures (typically 325–365 K) are also shown by dotted lines. The figure includes the spectra [Fig. 2(d)] for PMMPS which has a disordered backbone even at low temperatures. The respective OA spectra show intense peaks which have been assigned to the lowest singlet exciton states associated with the interband transitions (*vide infra*). The position of the absorption peaks critically depends on the backbone conformation: 3.4 eV for *trans*-planar PDHS, 3.7 eV for TGTG′ PDTDS, and 4.0 eV for $\frac{7}{3}$ helical PDBS. Such a conformation-dependent change of the optical gap may reflect the delocalized nature of σ-electron states. In fact, the tendency observed here is in accord, at least qualitatively, with theoretical predictions based on the band calculations.[2,17]

The OA spectra for the disordered conformations of PDHS, PDTDS, and PDBS above the critical temperature for the phase transition are all very similar and compare well with that for PMMPS which is similarly disordered. A broader spectral profile for the disordered conformation is perhaps due to inhomogeneous broadening effects. Beyond the phase transition, the lowest singlet exciton band shifts to higher energy (3.9 eV) for the *trans*-planar and TGTG′ conformations [see Figs. 2(a) and 2(b)], suggesting a decrease in the delocation of σ electrons along the polymer backbone caused by the conformational change. In contrast, the lowest exciton band

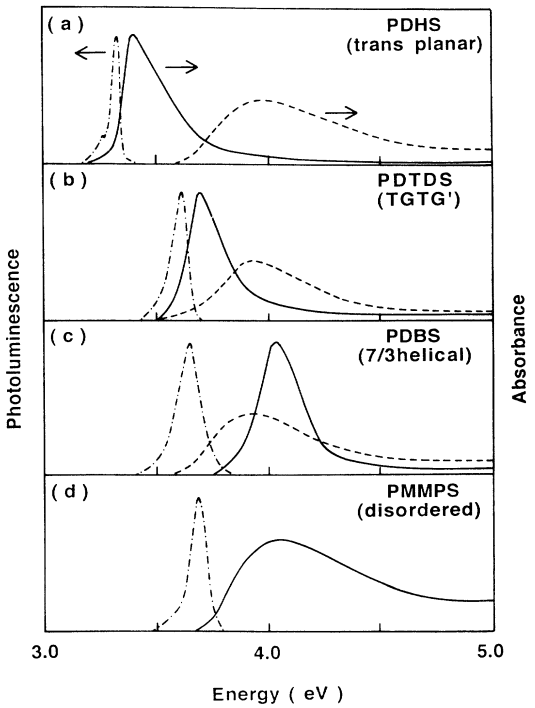

FIG. 2. Ordinary absorption (solid line) and photoluminescence (dashed-dotted line) spectra in thin films of polysilanes at 77 K; (a) *trans*-planar PDHS, (b) TGTG′ PDTDS, (c) $\frac{7}{3}$ helical PDBS, and (d) disordered PMMPS. Dashed lines represent absorption spectra for the respective polysilanes above the phase-transition temperatures.

for the $\frac{7}{3}$ helical conformation was observed to shift to lower energy upon the conformational transition to the disordered form.

There is also a clear difference in spectral features of photoluminescence between the $\frac{7}{3}$ helical chains and the *trans*-planar or TGTG′ chains. The PL peaks for the *trans*-planar and TGTG′ chains appear at nearly the same energies relative to the OA peaks with essentially no Stokes shift and no vibrational structure. Such a resonance emission implies weak exciton-lattice interaction in polysilanes, which is rather exceptional for conjugated polymers. An apparent Stokes shift is observed in PL spectra for the ordered $\frac{7}{3}$ helical conformation: The PL peak shows up around 3.6 eV near the edge of the low-energy tail of the OA spectrum. Such features are often observed in semiconductors and molecular crystals showing an indirect gap or indirect exciton. In the $\frac{7}{3}$ helical PDBS, the indirect exciton is likely to be located in the lower energy region (3.6–3.7 eV) than the direct exciton (4.0 eV) which appears as the OA peak. This is perhaps because the electronic band dispersion is significantly folded in the **k**-space due to the long-period nature of the $\frac{7}{3}$ helical conformation.

In contrast to the OA spectrum, the PL spectrum in the disordered conformation is as sharp as in other ordered conformations and its peak is observed at the lower edge of the OA band. As a primary process for the PL in the disordered chain, the photogenerated exciton seems to migrate and relax to the portion of the chain with the lower exciton energy (i.e., the OA tail region), and then undergo the radiative recombination.

IV. ONE-DIMENSIONAL EXCITON STATES OF TRANS PLANAR POLYSILANES

A. Spectra of two-photon and electroabsorption

Of the polysilanes investigated, PDHS may be viewed as the simplest microwire with a regular structure of the *trans*-planar type. Let us summarize here the linear and nonlinear optical data which are important in unraveling features of the exciton states characteristic of one-dimensional semiconductors. In Fig. 3 we show the one-photon absorption (a solid line) and two-photon absorption (TPA) (a dashed line) spectra (upper part) as well as the electroabsorption (EA) spectra (lower part) for PDHS films with *trans*-planar conformation at 77 K. The high-energy TPA curve represented by open circles in the figure shows the result reported by Soos and Kepler.[10] The lower-energy TPA spectrum of the present sample is essentially in agreement with the result reported previously by Thorne *et al.*[8] The value of $-\Delta T/T$ for the EA spectra represents the differences between the absorption with and without the electric field, where ΔT is the change in transmittance (T) caused by the electric field.

The EA structure around 3.4 eV obviously corresponds to the exciton peak in the OA spectra. The EA peak corresponds with the calculated curve of the first energy derivative of the original OA spectrum, implying the field-induced energy shift (Stark shift) of the exciton resonance energy. In addition, the EA spectra reveal several important excited states which are difficult to detect by OA spectroscopy. The EA peak at 4.22 eV and subsequent oscillatory structure (indicated by an arrow) have

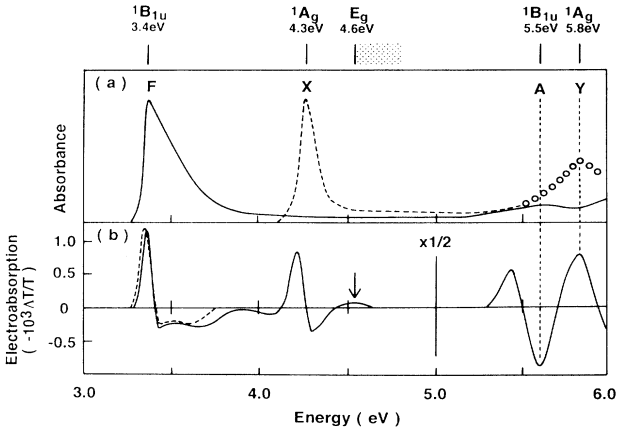

FIG. 3. Spectra of (a) one-photon (solid line) and two-photon (dashed line) absorption and (b) electroabsorption in thin films of PDHS with *trans*-planar conformations at 77 K. Dashed lines represent the first energy derivative curve of the OA peak *F*. Open circles in (a) indicate data of two-photon absorption spectra reported by Soos and Kepler[10] which are normalized to the presently observed data at 4.27 eV.

no counterpart in the OA spectrum, but appear to correspond to the TPA peak (X) observed at nearly the same position. In addition to these features, intense EA signals (denoted as A and Y) were observed in the higher energy region. These two features also appear to correspond well with the OA and TPA peaks. In the following section, we first discuss the low-energy features observed below 5 eV which are relevant to the one-dimensional excitonic structure associated with interband transitions.

Before proceeding to the interpretation of the rather complicated (but very informative) EA spectra, let us briefly discuss the nature of the exciton states, F and X, which were observed in the OA (one-photon) and TPA spectra, respectively, and hence should have different parities. In our previous publication,[11] we have assigned the observed one-photon (F) and two-photon (X) transitions below 4.5 eV in *trans*-planar polysilanes to the ground ($v=1$) and first excited ($v=2$) states of one-dimensional Wannier type excitons (see Fig. 4). Let us add here some arguments on the excitonic assignment previously assigned. In general, there may be different theoretical approaches to the problem of exciton structures observed in polysilanes. We have adopted the one-dimensional semiconductor model where only the final state interaction (Coulombic) between the excited electron and hole is explicitly taken into account. In other words, we assume that the electron correlation effect can be readily included in the one-electron band structure in the sense of the mean-field approximation. This theoretical approach contrasts with the quantum chemical ones which consider configuration interactions and multiexcitation processes. The latter is more rigorous but can be done only for a finite-length chain system.[10] The former weak-coupling model is based on the hypothesis that the one-electron band picture is a good starting point. Nevertheless, it gives an intuitive view in terms of a series of Wannier excitons and subsequent interband transitions which can be compared with the conventional pictures of inorganic semiconductors of higher dimensionality.

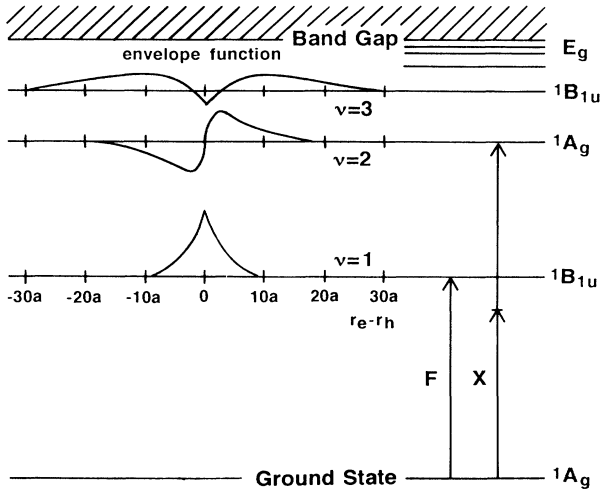

FIG. 4. Schematic envelope functions and level diagram for the Wannier exciton structure in *trans*-planar polysilanes.

The Wannier type excitons in one-dimensional semiconductors are relevant, in the spirit of the effective-mass approximation, to the problem of a one-dimensional hydrogen atom,[18] since the bound or unbound electron-hole pair is analogous to the electron-proton composite (hydrogen) system. The hydrogenic exciton model in one dimension predicts that the exciton series have alternating even and odd envelope functions (electron-hole internal wave functions).[19,20] In the D_{2h} symmetry of *trans*-planar polysilanes (PDHS), the symmetry of a total wave function including Wannier functions should be either $^1B_{1u}$ with an even envelope function or ^1A_g with an odd one. In particular, the ^1A_g state has a character of the charge-transfer exciton, the envelope function of which is antisymmetric with a node at the origin (see Fig. 4). Then, the observed one-photon (F) and two-photon (X) allowed excitons can be assigned to the ground ($^1B_{1u}$) and first excited (^1A_g) states of the one-dimensional excitons, respectively.

B. Analysis of electroabsorption spectra in terms of one-dimensional Wannier exciton model

On the basis of the Wannier exciton model, the origin of the electric-field effect on the absorption spectra can be discussed as follows. The Stark shift of the lowest $^1B_{1u}$ exciton (peak F) is induced by mixing with the near-lying ^1A_g exciton in the electric field. Therefore, the two-photon allowed ^1A_g exciton is activated by the electric field as seen in the field-induced signal for the X exciton. More generally, the external electric field causes the mixing between various $^1B_{1u}$ and ^1A_g states via their matrix elements of transition dipoles.

We show in Fig. 5 a comparison of the experimental OA, EA, and TPA spectra in PDHS (77 K) below 5 eV with the calculated ones. The spectra shown in Figs. 5(b) and 5(c) were calculated assuming the three- and four-level systems, respectively. In the three-level model, we assume only the two excited states (in addition to the ground state g), i.e., the $^1B_{1u}$ and ^1A_g states which correspond to the ground ($v=1$) and first excited ($v=2$) states of the one-dimensional excitons. These two exciton states can reproduce the observed one-photon (OA, a dashed line) and two-photon (TPA, a dashed-dotted line) spectra as well as the Stark shift of the $v=1$ exciton, if the transition dipole of x_{12} is assumed to be finite. However, this three-level model can never, even qualitatively, reproduce the observed feature of the EA spectrum around 4.2 eV. The experimental EA curve shows a much more pronounced feature around the exciton X than one calculated in terms of the three-level model. (As a measure for the transition strength of the field-activated state (e.g., X exciton), we use its relative magnitude to that of the Stark shift signal of the $v=1$ state.)

An unusual transition intensity of the field-activated X exciton (relative to the Stark shift signal) and an additional EA structure around the X exciton indicate that there should be additional excited states which are located nearby and mix with the X ($v=2$) exciton in the external field. To mimic this situation, we assume an additional $^1B_{1u}$ exciton ($v=3$) located above the X ($v=2$) exciton.

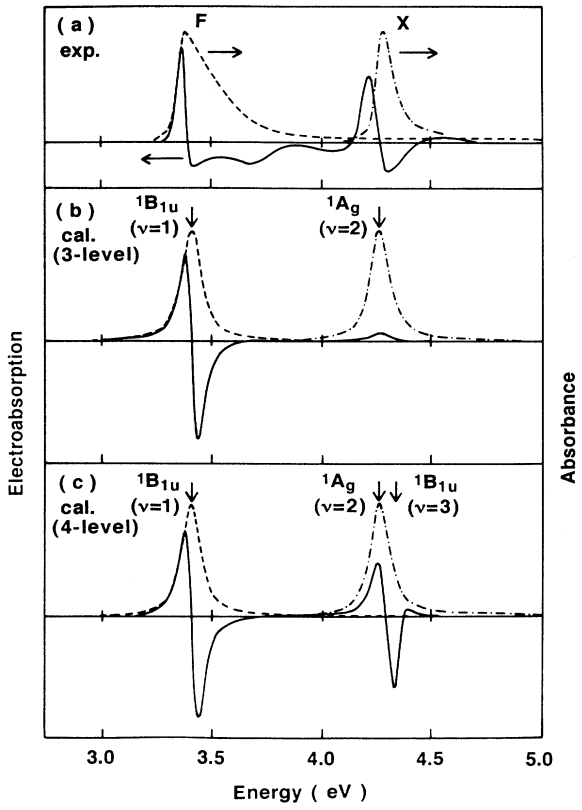

FIG. 5. (a) Observed and (b) and (c) calculated spectra for electroabsorption (solid line) and one-photon (dashed line) and two-photon (dashed-dotted line) absorption spectra in PDHS. For the calculation, the different orders of the exciton diagrams are used; the $v=1$ ($^1B_{1u}$) and $v=2$ (^1A_g) exciton states for (b) the three-level model and additionally the $v=3$ ($^1B_{1u}$) exciton state for (c) the four-level model. The parameters used in the calculation are listed in Table II.

We show in Fig. 5(c) the calculated results for such a four-level system, in which the $v=1-3$ exciton energies are indicated by arrows. (Optimized parameters for the transition dipoles used in the calculation were listed in Table II.) Assuming this model, there is another strong channel for the field-induced mixing between the ^1A_g ($v=2$) state and the $^1B_{1u}$ ($v=3$) state. The calculated results compare well with the observed feature shown in Fig. 5(a). The field-induced mixing between the $v=2$ and 3 exciton states enhances the activation of the $v=2$ exciton as well as the deactivation of the $v=3$ exciton. Such a combined effect is the origin of the observed oscillatory EA signal around the X exciton as shown in Fig. 5(a). The reason why the higher-lying $^1B_{1u}$ (e.g., $v=3$) exciton can be hardly detected by OA spectroscopy but easily by the EA spectroscopy is as follows: The transition moment x_{g3} for the one-photon transition should be small as compared with x_{g1}, which is typical for the higher-lying exciton states with extended envelope functions in one dimension. However, the matrix element x_{23} responsible for the field-induced mixing between the $v=2$ and 3 excitons can be large (see Table II). For the same reason, such higher-lying $^1B_{1u}$ transitions as the $v\geq 3$ exciton are expected to be detected by various types of nonlinear spectroscopy. In fact, the $v\geq 3$ $^1B_{1u}$ states have also been detected as the three-photon resonant states in the excitation spectroscopy of third harmonic generation (*vide infra*).[21]

One may feel that the adopted parameter settings are somewhat arbitrary. However, the present simulation for the excitonic structures is based on the following reasoning. As mentioned above, the higher-lying one-photon allowed ($^1B_{1u}$) states show much weaker transition dipoles than the lowest exciton (F), yet rather large transition dipoles from the nearby ^1A_g states (e.g., X exciton). (We will see the microscopic reasoning of variation in transition dipoles in the latter part of this section.) It was demonstrated in the present calculation by varying the excitonic level orders that there exist a series of the one-dimensional Wannier exciton states with alternating even and odd envelope functions. In fact, the agreement between the observed and simulated EA curves was found to be further improved, in particular for the hump on the high-energy side around 4.5 eV in the observed EA spectrum, if a next higher-lying ^1A_g ($v=4$) state is included in the calculation.

Such a Wannier-like series of exciton states can be in fact obtained by a calculation based on a microscopic weak-coupling model. One of the present authors (S.A.) and his coworkers have recently carried out numerical calculations for a finite chain using a simple tight-binding model of polysilane.[22] We apply the same model to the analysis of the EA spectra not only in *trans*-planar PDHS as shown in Ref. 22, but also for other polysilanes with different backbone conformations. Here, let us briefly summarize the theoretical framework.

The model is based on the Sandorfy C approximation,[23] in which only two sp^3 orbitals of each Si atom pointing to neighboring Si atoms are taken into account, rendering the model analogous to those for conjugated polymers such as polyacetylene.[24,25] Within the semiempirical Pariser-Parr-Pople-type parametrization, the essential features of the model are as follows: the vicinal and geminal transfer energies $-t_v$ and $-t_g$ ($t_v > t_g > 0$); the Coulomb repulsion V_{ij} between ith and jth orbitals along the chain. Although the Ohno potential is often used for V_{ij}, we use a simpler form by Pople,[26] $V_{ij}=V/|i-j|$ for $i\neq j$, and $V_{ii}=U$, so that the model has as few parameters as possible. The essential features of the calculated results do not depend on the detailed form of the potential. V is the Coulomb repulsion between nearest-neighbor orbitals and may be written as $V=2e^2/\epsilon a$ using the electron charge e, the dielectric constant ϵ, and the lattice constant a.

The exciton states can be calculated by using a standard single configuration-interaction method.[27] We first obtain the ground state of the one-electron Hamiltonian and construct the excited states of a single electron-hole pair from the ground state. Then the matrix of the total Hamiltonian within the single-excitation subspace is diagonalized. Actual calculations have been carried out numerically for a chain of 500 atoms (1000 orbitals).

TABLE II. Optimized parameters for the exciton states ($\nu=1-3$) of the *trans*-planar PDHS. See text and the caption of Fig. 5. Values in parentheses are optimized parameters for the transition dipoles used in the calculation based on the tight-binding model.

Parameter	
Γ	0.05 eV
E_1	3.40 eV
E_2	4.26 eV
E_3	4.34 eV
x_{g3}/x_{g1}	0.07 (0.08)
x_{23}/x_{21}	−3.0 (−2.8)

After obtaining all the necessary dipole matrix elements between ground and excited states as well as among excited states, the linear and third-order nonlinear susceptibilities $\chi^{(3)}$ are calculated by using a standard formula[28] summing over all relevant dipole matrix elements and taking lifetime broadening into account. Note that the TPA (two-photon absorption) and the EA (electroabsorption) spectra correspond to the imaginary parts of $\chi^{(3)}(-\omega;\omega,-\omega,\omega)$ and $\chi^{(3)}(-\omega;\omega,0,0)$, respectively.

The results for the complete calculation of the one-dimensional Wannier exciton states based on such tight-binding Hamiltonians are shown in Fig. 6. We assumed a lifetime broadening of 0.05 eV for the lowest $^1B_{1u}$ ($\nu=1$) and ^1A_g ($\nu=2$) states, while a large value, 0.15 eV, was used for all the higher states, which can readily decay to $K\neq 0$ states of lower exciton branches by emitting phonons or by defect scattering. The calculations could reproduce consistently all the observed exciton spectra, e.g., OA, TPA, and EA spectra in PDHS using an appropriate set of parameters (see Table IV). It is to be noted that the transition dipoles used in the model calculation for Fig. 5(c) were close to the values evaluated for PDHS polysilanes in the present microscopic calculation, as listed for comparison in Table II.

According to the present approach to the excitonic structures, the conventional band-to-band transition is considered to be located at the extrapolated ($\nu=\infty$) position. Judging from the rapidly converging nature of the exciton energy with the quantum number (ν) and also by comparison of the observed EA spectra with the calculated one, the interband edge is considered to be around 4.6 eV, i.e., around the higher-lying broad maximum of the EA spectrum. Therefore, the present analysis shows that the binding energy of the lowest ($\nu=1$) exciton state can be as large as 1.2 eV (see Table III). Such a large binding energy is inherent in the one-dimensional electron-hole system, which also explains why the one-photon spectral weight is so concentrated on the lowest exciton.[29]

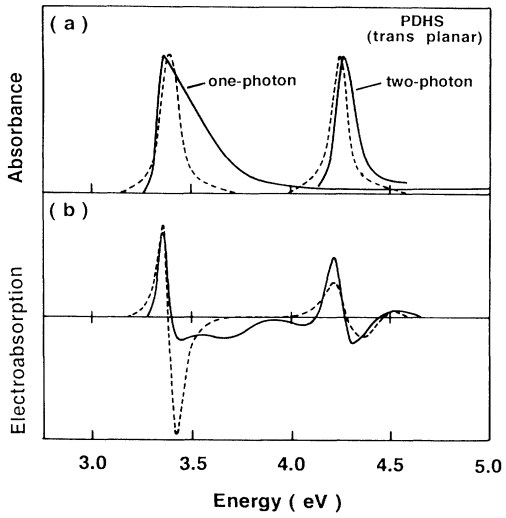

FIG. 6. Observed (solid line) and calculated (dashed line) spectra for (a) one-photon and two-photon absorption and (b) electroabsorption spectra in PDHS. The parameters used in the calculation are listed in Table IV.

Recently, Hasegawa *et al.*[21] have applied the same scheme for the excitonic structures as adopted here to the analysis of the three-photon excitation spectra for the third harmonic generation in *trans*-planar PDHS and obtained excellent agreement between the experimental and calculated spectra for $\chi^{(3)}(-3\omega;\omega,\omega,\omega)$. In particular, they observed the clear structures in $\chi^{(3)}$ spectra due to the three-photon resonance with the $\nu\geq 3$ exciton.

C. Possible origins of the higher-lying two-photon band

Coming back to Fig. 3, we add some comments on another exciton series observed above 5.5 eV. It was demonstrated in a previous study on highly oriented PDHS films[30] that the one-photon absorption band A at 5.5 eV is polarized parallel to the Si backbone as is the case for the lowest exciton F and hence can be assigned to the exciton associated with different σ-σ^* interband transitions. On the high-energy side of the A band, the two-photon absorption band was observed by Soos and

TABLE III. Observed energies of the Wannier type excitons and band gap (E_g) in various polysilanes.

	$^1B_{1u}$ ($\nu=1$) (eV)	^1A_g ($\nu=2$) (eV)	$^1B_{1u}$ ($\nu=3$) (eV)	E_g (eV)
PDHS (*trans*-planar)	3.38	4.27	4.30	4.6
PDTDS (TGTG′)	3.63	4.62	4.78	5.1
PDBS ($\frac{7}{3}$ helical)	4.00	4.86	4.94	5.3
PMMPS[a] (disordered)	~4.0	~4.9	~	~

[a]Taken at the peak.

Kepler,[10] as shown by open circles in Fig. 3. In accord with these one-photon ($^1B_{1u}$) and two-photon (^1A_g) transitions, a pronounced EA signal is observed in the corresponding energy region. The shape of the EA spectrum in this region can be reproduced by assuming the field-induced mixing effect between the $^1B_{1u}$ (5.5 eV) and ^1A_g (5.8 eV) states. It would be natural to assign these two states to another Wannier exciton series ($v'=1$ and 2) associated with the higher-lying interband transitions. As argued in previous studies,[10,12] however, we should not discard the possibility of the two-electron excitation configuration for the character of the Y (^1A_g) exciton at 5.8 eV. Considering that the energy of the Y exciton is not too much different from twice the lowest F ($^1B_{1u}$) exciton energy ($3.4\times2=6.8$ eV), it may be anticipated there is some configuration mixing of the double excitation of the F exciton with the Y exciton. If such a character is strong enough for the Y exciton, it may be viewed as a biexciton (or molecular exciton) on the Si chain. To confirm this possibility, further study, in particular experimental evaluation of the transition dipole between the F($^1B_{1u}$) exciton and Y(^1A_g) exciton, would be necessary.

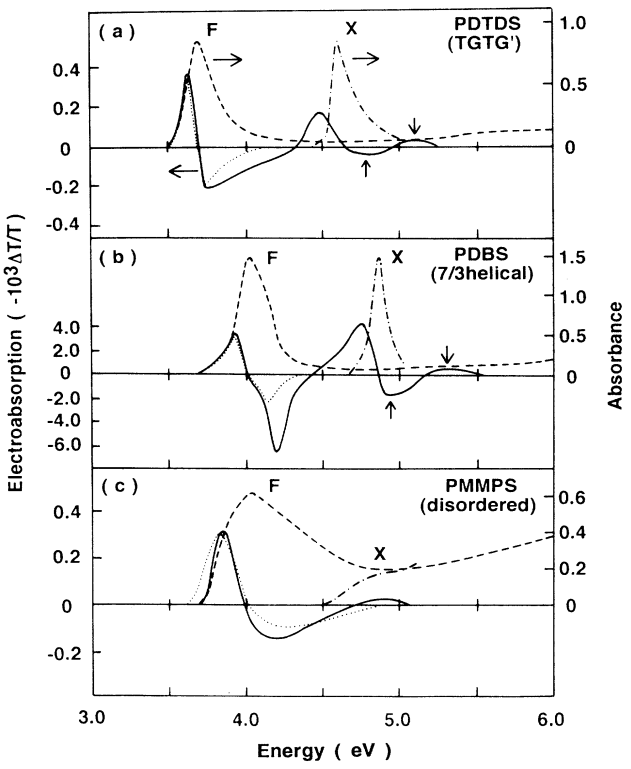

FIG. 7. Electroabsorption (solid line), ordinary absorption (dashed line), and two-photon absorption (dashed-dotted line) spectra in thin films of polysilanes at 77 K; (a) TGTG' type PDTDS, (b) $\frac{7}{3}$ helical PDBS, and (c) disordered PMMPS. Dotted lines represent the first energy derivative curve of the OA peak F for each backbone conformation. Arrows indicate the estimated positions of the $v=3$ ($^1B_{1u}$) exciton and the band gap (E_g).

V. EXCITON STATES OF POLYSILANES WITH VARIOUS BACKBONE CONFORMATIONS

EA spectra (at 77 K) in thin films of polysilanes with the other backbone conformations, namely TGTG' (PDTDS), $\frac{7}{3}$ helical (PDBS), and disordered (PMMPS), are shown in Fig. 7 together with their OA and TPA spectra. As reported previously,[11] the distinct two-photon absorption band (X) observed at 0.9–1.0-eV higher energy above the one-photon allowed singlet exciton (F) is common to various polymer conformations. These exciton series can be likewise assigned to the ground ($v=1$) and first excited states ($v=2$) of the one-dimensional Wannier exciton.

The EA spectra of these polysilanes also show very similar features to those of PDHS apart from the energy positions. The Stark shift signals are observed in the same energy region of the OA peaks due to the lowest singlet (F) excitons, which are again well reproduced by the calculated curves for the first energy derivative of the original OA spectra. In addition, the characteristic EA signals corresponding to the two-photon allowed X excitons are similarly observed accompanying the higher-lying humps (indicated by arrows) in PDTDS and PDBS. Such oscillatory structures in the EA spectra indicate again that there are hidden higher excited states on the higher-energy side of the X ($v=2$) exciton. We can approximately assign the energy around the EA minimum to the deactivation of the $v=3$ exciton and the subsequent rise of the EA signal to the higher-lying $v\geq4$ excitons or the onset of the electron-hole continuum.

All the observed exciton spectra can be rationalized with the theoretical model by reducing the geminate transfer energy t_g. In fact, the spectra for PDTDS and PDBS can be reproduced theoretically as shown in Fig. 8 by choosing an appropriate t_g and slightly adjusting V (see Table IV). The broadening parameters are the same as in the case of PDHS. We have not changed t_v and U, which are considered to be relatively independent of the conformation. The origin of the conformation dependence of t_g is beyond the scope of the present semiempirical approach and should be clarified by a first-principle calculation. The agreement between the experimental and theoretical results is satisfactory, supporting again the present one-dimensional exciton model.

Concerning PMMPS with the disordered conformation in Fig. 7(c), only the blurred signal was observed in the EA spectrum due to the inhomogeneously broadened feature, yet the field activation of the $v=2$ exciton state

TABLE IV. Parameters used for the calculation of one-dimensional exciton spectra (Figs. 6 and 8) of PDHS (*trans*-planar), PDTDS (TGTG'), and PDBS ($\frac{7}{3}$ helical).

	PDHS (*trans*-planar)	PDTDS (TGTG')	PDBS ($\frac{7}{3}$ helical)
t_v	2.50 eV	2.50 eV	2.50 eV
t_g	1.25 eV	1.10 eV	0.96 eV
U	5.25 eV	5.25 eV	5.25 eV
V	2.63 eV	2.63 eV	2.53 eV

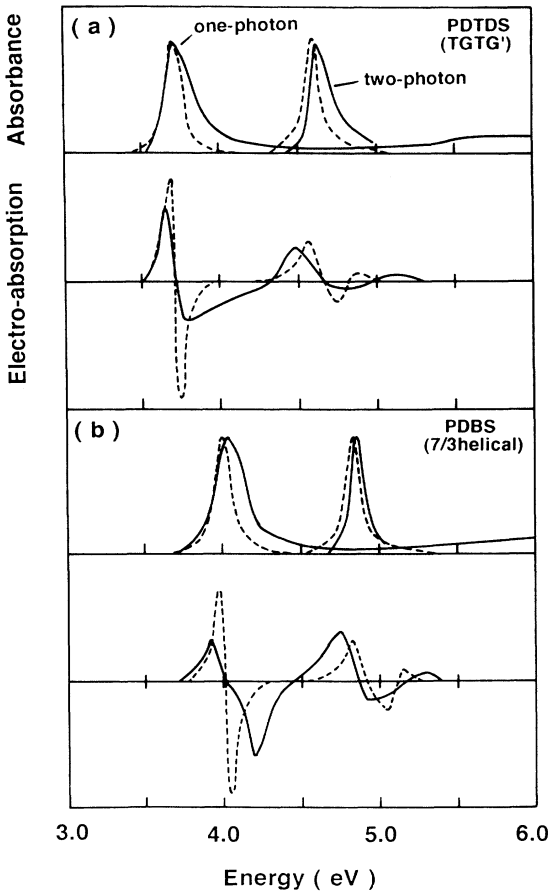

FIG. 8. Observed (solid line) and calculated (dashed line) spectra for one-photon and two-photon absorption and electroabsorption spectra in (a) PDTDS and (b) PDBS. The parameters used in the calculation are listed in Table IV.

was still observed at nearly the same position of the two-photon absorption band X. In Table III, we have listed the resonance ($\mathbf{k}=0$) energies of the $\nu=1$, 2, and 3 excitons and the band-gap energy (E_g), which was tentatively taken as the position of the EA hump signal, indicated by an arrow in Fig. 6. [The values for PDBS with a $\frac{7}{3}$ helical structure should be taken as those for the direct excitons and direct gap, since the helical chain is likely to show lower-lying indirect ($\mathbf{k}\neq 0$) excitons and band gap as mentioned earlier.] The binding energies of the $\nu=1$ (ground state) exciton is as large as 1.1–1.5 eV for these regular polysilanes, reflecting the one-dimensional nature of the electronic structures.

Incidentally, the one-photon (A) and the two-photon (Y) bands observed in PDHS films were not observed below 6 eV for the polysilanes with a TGTG' or $\frac{7}{3}$ helical conformation. On the other hand, the chain-polarized band corresponding to the A band has been observed for poly(di-*n*-hexylgermane),[31] a Ge-analog of PDHS, also with the *trans*-planar conformation. Therefore, the higher-lying exciton series, A and Y bands, are characteristic of the *trans*-planar conformations. In accord with this observation, the strong EA signals corresponding to the A ($^1B_{1u}$) and Y (^1A_g) bands were observed to totally disappear upon the order-disorder transition in PDHS chains.[14]

VI. SUMMARY

We have investigated the electronic states for a variety of polysilanes with *trans*-planar, alternating *trans-gauche* (TGTG' type), $\frac{7}{3}$ helical, and disordered backbone conformations by measurements of one-photon and two-photon absorption, photoluminescence, and electroabsorption spectra. In each polysilane, a series of one-dimensional Wannier exciton states and band-to-band transitions have been unraveled from the direct measurement of one-photon and two-photon absorption spectra as well as from the analysis of the electroabsorption spectra. The calculations based on the one-dimensional Wannier exciton model can reproduce the observed features of one-photon and two-photon absorption spectra as well as those of electroabsorption spectra. The large binding energies (1.2–1.5 eV) of the lowest singlet exciton and the existence of alternating series of $^1B_{1u}$ and ^1A_g states are inherent in the one-dimensional semiconductors or ultimate quantum wires like polysilanes.

Another unique feature for the one-dimensional excitons in polysilanes is the existence of resonant luminescence of the excitons with high quantum efficiency. This is in contrast to the observation that the one-dimensional excitons in π-conjugated polymers mostly undergo self-trapping by strong exciton-lattice interaction. Furthermore, most of the conventional Si frameworks are poorly luminescent. Exciton recombination with high quantum efficiency seems to be a consequence of the extremely weak exciton-lattice interaction on the Si chains and of the wide-gap nature. Among various conformations of Si chains, PDBS with the $\frac{7}{3}$ helical conformation may have the indirect excitons, which will be of another interest from the viewpoint of the dynamics of the lowest indirect excitons in one-dimensional chains.

ACKNOWLEDGMENTS

The authors are grateful to T. Hasegawa, Y. Iwasa, T. Koda, W. P. Su, and M. Schreiber for enlightening discussions. The present work was supported by a Grant-In-Aid for Scientific Research from Ministry of Education, Science and Culture, Japan, and by Foundation from the New Energy and Industrial Technology Development Organization (NEDO), Japan.

*Present address: Central Research Laboratory, Hitachi Ltd., Kokubunji, Tokyo 185, Japan.
†Present address: Photodynamics Research Center, The Institute of Physical and Chemical Research (RIKEN), Aoba-ku, Sendai 989-32, Japan.

[1] K. Takeda and K. Shiraishi, Phys. Rev. B **39**, 11 028 (1989).
[2] J. W. Mintmire, Phys. Rev. B **39**, 13 350 (1989).
[3] R. D. Miller and J. Michl, Chem. Rev. **89**, 1359 (1989).

[4]F. Kajzar, J. Messier, and C. Rosilio, J. Appl. Phys. **60**, 3040 (1986).
[5]L. A. Harrah and J. M. Zeigler, Macromolecules **20**, 601 (1987).
[6]R. G. Kepler, J. M. Zeigler, L. A. Harrah, and S. R. Kurtz, Phys. Rev. B **35**, 2818 (1987).
[7]J. M. Zeigler, L. A. Harrah, and A. W. Johnson, SPIE Adv. Resist Technol. **539**, 166 (1985).
[8]J. R. G. Thorne, Y. Ohsako, J. M. Zeigler, and R. M. Hochstrasser, Chem. Phys. Lett. **162**, 455 (1989).
[9]F. M. Schellenberg, R. L. Byer, and R. D. Miller, Chem. Phys. Lett. **166**, 331 (1990).
[10]Z. G. Soos and R. G. Kepler, Phys. Rev. B **43**, 11 908 (1991).
[11]Y. Moritomo, Y. Tokura, H. Tachibana, Y. Kawabata, and R. D. Miller, Phys. Rev. B **43**, 14 746 (1991).
[12]H. Tachibana, Y. Kawabata, S. Koshihara, and Y. Tokura, Solid State Commun. **75**, 5 (1990).
[13]R. G. Kepler and Z. G. Soos, Phys. Rev. B **43**, 12 530 (1991).
[14]H. Tachibana, Y. Kawabata, S. Koshihara, and Y. Tokura, Synth. Met. **41**, 1385 (1991).
[15]P. Trefonas III, P. I. Djurovich, X. H. Zhang, R. West, R. D. Miller, and D. Hofer, J. Polym. Sci., Polym. Lett. Ed. **21**, 819 (1983).
[16]M. Fujino and H. Isaka, J. Chem. Soc., Chem. Commun. **1989**, 466 (1989).
[17]N. Matsumoto and H. Teramae, J. Am. Chem. Soc. **113**, 4481 (1991).
[18]R. Loudon, Am. J. Phys., **27**, 649 (1959).
[19]P. Pugh, Mol. Phys. **26**, 1297 (1973).
[20]S. Abe, J. Phys. Soc. Jpn. **58**, 62 (1989).
[21]T. Hasegawa, Y. Iwasa, H. Sunamura, T. Koda, Y. Tokura, H. Tachibana, M. Matsumoto, and S. Abe, Phys. Rev. Lett. **69**, 668 (1992).
[22]S. Abe, M. Schreiber, and W. P. Su, Chem. Phys. Lett. **192**, 425 (1992).
[23]C. Sandorfy, Can. J. Chem. **33**, 1337 (1955).
[24]Z. G. Soos and G. W. Hayden, Chem. Phys. **143**, 199 (1990).
[25]S. Abe, M. Schreiber, W. P. Su, and J. Yu, Phys. Rev. B **45**, 9432 (1992).
[26]J. A. Pople, Trans. Faraday Soc. **46**, 1375 (1953).
[27]R. S. Knox, *Theory of Excitons* (Academic, New York, 1963), Suppl. 5.
[28]B. J. Orr and J. F. Ward, Mol. Phys. **20**, 513 (1971).
[29]T. Ogawa and T. Takagahara, Phys. Rev. B **43**, 14 325 (1991).
[30]H. Tachibana, Y. Kawabata, S. Koshihara, T. Arima, Y. Moritomo, and Y. Tokura, Phys. Rev. B **44**, 5487 (1991).
[31]H. Tachibana, Y. Kawabata, A. Yamaguchi, Y. Moritomo, S. Koshihara, and Y. Tokura, Phys. Rev. B **45**, 8752 (1992).